

ANGULAR CORRELATIONS: Hf 177

A PERTURBED ANGULAR CORRELATION  
STUDY OF  
HAFNIUM 177

by

WALTER HERBERT BROOKER, B.SC.

A Thesis

Submitted to the Faculty of Graduate Studies  
in Partial Fulfilment of the Requirements  
for the Degree  
Master of Science

McMaster University

October 1967

MASTER OF SCIENCE (1967)  
(Physics)

McMASTER UNIVERSITY  
Hamilton, Ontario.

TITLE: A Perturbed Angular Correlation Study of Hafnium  
177 .

AUTHOR: Walter Herbert Brooker, B.Sc. (McMaster University)

NUMBER OF PAGES: vi, 53

SCOPE AND CONTENTS:

Lutetium 177 ions were implanted in iron and nickel foils using a mass separator. The rotations of the angular correlation pattern caused by the hyperfine fields acting on the implanted nuclei were measured for the 71-250 keV and the 208-113 keV cascades in the beta-decay product Hafnium 177. Using measured data, the g-factor for the 250 keV spin 11/2, second excited state in  $\text{Hf}^{177}$  was determined, as were the internal fields acting on the  $\text{Hf}^{177}$  impurity in iron and nickel.

The results are as follows:

$$g_{11/2} = 0.277 \pm 0.080$$

$$H_{\text{Fe}}(\text{int}) = -133 \pm 7 \text{ kOe}$$

$$H_{\text{Ni}}(\text{int}) = -58.6 \pm 8 \text{ kOe}$$

### ACKNOWLEDGEMENTS

The author wishes to express his gratitude to his supervisor, Dr. J. A. Cameron, for his guidance, assistance and friendly advice during the course of this work.

Thanks are due also to the other members of the group, J. Murray, T. A. McMath and M. B. Byrnes for their assistance, and to the National Research Council for financial support.

Finally, thank you to my wife, Mary-Joan, for her large understanding and help during the work and writing.

## TABLE OF CONTENTS

<u>CHAPTER</u>		<u>Page</u>
I	INTRODUCTION	1
II	ANGULAR CORRELATION THEORY	4
	2.1 Angular Correlations	4
	2.2 Perturbed Angular Correlations	8
III	FERROMAGNETIC MATERIALS AND HYPERFINE FIELDS	10
	3.1 Introduction	10
	3.2 Ferromagnetism	11
	3.3 Hyperfine Fields	13
IV	THE COLLECTIVE MODEL AND NUCLEAR MOMENTS	15
	4.1 Introduction	15
	4.2 The Collective Model	17
	4.3 Magnetic Moments	19
	4.4 Multipole Transitions	22
V	APPARATUS	25
VI	EXPERIMENTAL	32
	6.1 Angular Correlations	32
	6.2 Sources	32
	6.3 Perturbed Angular Correlations	36
VII	RESULTS	38
	7.1 Angular Correlations	38
	7.2 Measurements of g-factors	42
	7.3 Hyperfine Fields	43
	7.4 Discussion	44

TABLE OF CONTENTS (CONTINUED)

<u>CHAPTER</u>		<u>Page</u>
VII (CONT'D)	7.4.1 Hyperfine Fields	44
	7.4.2 g-factors	46
	7.5 Summary	50
BIBLIOGRAPHY		52

## LIST OF ILLUSTRATIONS

<u>FIGURE</u>	<u>TITLE</u>	<u>Page</u>
1	Simple gamma decay	5
2	Coupling scheme for highly deformed nuclei	20
3	Data collection system	27
4	Pulse routing system	28
5	Coincidence spectra showing spectra in coincidence with windows A and B	33
6	Coincidence spectra showing spectra in coincidence with windows C and D	34
7	Saturation test on the iron sample	37
8	The relevant part of the $^{177}\text{Lu}$ decay scheme	39
9	The angular correlation pattern for the 208-113 cascade	40
10	The angular correlation pattern for the 71-250 cascade	41
11	Hyperfine field versus host magnetic moment	45

## CHAPTER I

### INTRODUCTION

The theory of angular correlations of gamma rays produced in nuclear reactions was introduced by Hamilton in 1940 [Hamilton, 1940], and Goertzel examined the theory with special regard to perturbations on the intermediate state [Goertzel, 1946]. The first successful experiments were carried out by Brady and Deutsch [1947]. However, the development of scintillation detectors and their use with fast coincidence circuits was necessary before the field of gamma-gamma correlations could contribute to the knowledge of the nucleus on a large scale. The effects of extra-nuclear fields on the nucleus were first investigated by the Zurich group [Aeppli et al. 1951].

The experimental technique consists of measuring coincidences between gamma rays of a cascade in a decaying nucleus as a function of the angle between two detectors, one of which detects each gamma ray.

The angular correlation pattern produced by such a measurement may now be perturbed by a large magnetic field, external to the nucleus. The effect of this per-

turbing field is discussed in Chapter II, where it is shown that the g-factor for the intermediate state in the cascade may be obtained by this technique.

The first work done with perturbed angular correlations made use of large external fields produced by electromagnets. Since the size of the measured effect depends on the magnetic field used and the lifetime of the intermediate state, the use of electromagnets set a lower limit on the lifetime of such states at about  $10^{-10}$  seconds.

In recent years, the use of the considerably larger magnetic fields at the nuclei of impurities in ferromagnetic alloys has lowered the minimum lifetime available for study.

One major requirement of this technique is that the atoms whose nuclei are being studied must be capable of forming alloys with ferromagnetic materials such as iron, cobalt and nickel. In the case of lutetium, the subject of this investigation, this alloying was not possible; according to the Hume-Rothery criteria for size and electronegativity, lutetium and iron, nickel or cobalt are extremely unlikely to form a solid solution [Hume-Rothery, 1947].

Hence, a different means of placing the lutetium nuclei at the lattice sites of iron and nickel was adopted. The isotope lutetium-177, prepared in the Atomic Energy

Company's reactor NRX, was implanted into iron and nickel foils by means of acceleration in a mass-separator, a technique used for  $^{133}\text{Xe}$  [Niesen, 1967], and for  $^{175}\text{Lu}$  by Deutch [1966].

The purpose of the investigation was to measure (a) the nuclear g-factor of the 250 keV second excited state of  $^{177}\text{Hf}$  and (b) the internal field on  $^{177}\text{Hf}$  in iron and nickel.

## CHAPTER II

### ANGULAR CORRELATION THEORY

#### 2.1 Angular Correlations

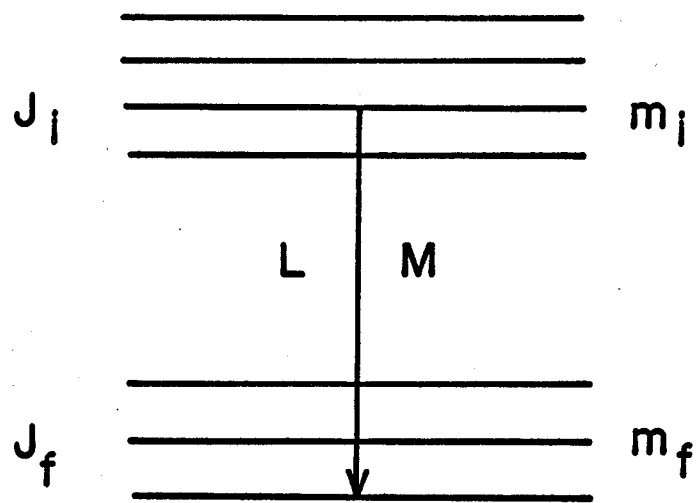
The probability of emission of a quantum of radiation or a particle by a radioactive nucleus depends in general upon the angle between the nuclear spin axis and the direction of radiation. It is necessary that the spins of the nuclei being observed not be randomly oriented if an anisotropic radiation pattern is to be observed. Such a situation may be arrived at by picking only nuclei whose spin lie in a preferred direction. If the nuclei decay through successive emission of two radiations  $R_1$  and  $R_2$ , the observation of  $R_1$  in a fixed direction  $\vec{k}_1$  chooses nuclei with spins in a preferred direction. Then, the succeeding radiation  $R_2$  may show an anisotropic angular correlation with respect to  $\vec{k}_1$ .

In such a decay, involving two gamma rays,  $\gamma_1$  and  $\gamma_2$ , the relative probability that  $\gamma_2$  is emitted into a solid angle  $d\Omega$  at an angle  $\theta$  with respect to  $\vec{k}_1$  is written  $W(\theta) d\Omega$ .

The directional distribution of radiation of all multipolarities is given by (figure 1)

Figure 1

Simple gamma decay



$$F_L(\theta) \propto \sum_{m_i m_f} P(m_i) G(m_i m_f) F_L^M(\theta)$$

where  $M = m_i m_f$ . Here,  $F_L^M(\theta)$  is the distribution function for radiation from a particular transition, and it may be calculated from the energy flow (Poynting vector) as a function of  $\theta$ .  $P(m_i)$  is the relative population of the levels and  $G(m_i m_f)$  is the relative transition probability for each component  $m_i \rightarrow m_f$ .

Now, it is of interest to write the angular correlation function for two gamma rays decaying in a cascade

$$I_i \rightarrow I \rightarrow I_f .$$

It is assumed that the gamma rays have multipolarities  $L_1$  and  $L_2$ .

Let the direction of the quantization axis lie along the direction of emission of the first gamma ray. Then the direction correlation between the two  $\gamma$ -rays becomes the directional distribution of the second  $\gamma$ -ray with respect to the z-axis. The theory then shows that the distribution may be written

$$W(\theta) = W(\vec{k}_1, \vec{k}_2) = \sum_{k \text{ even}} A'_{kk} P_k(\cos\theta)$$

It may be shown that the coefficients  $A'_{kk}$  break up into two factors, each depending on only one transition of the cascade; the  $A'_{kk}$  are usually normalized so that

$$A'_{00} = 1$$

It also follows from the theory that certain selection rules exist for the index  $k$ . These are

- i)  $k$  is an even integer
- ii)  $0 < k < \text{Min}(2I, 2L_1, 2L_2)$ .

Yang [1948] showed that this second rule follows from the invariance of the correlation process under rotation and inversion while the first holds when measurements are restricted to the directions of the radiations.

The correlation function may then be written as

$$W(\theta) = \sum_k A_k^{(1)} A_k^{(2)} P_k(\cos\theta)$$

where the superscripts refer to the two transitions. The coefficients  $A_k^{(1)}$  and  $A_k^{(2)}$  depend only upon the spins and multipolarities of the first and second transitions of the cascade respectively. These coefficients are tabulated [Ferentz and Rosenzweig, 1964].

These coefficients, when measured experimentally are subject also to correction due to the finite solid angle subtended by the detectors. The coefficients  $A'_{kk}$  which is measured, may be written

$$A'_{kk} = Q_{1k} A_k^{(1)} Q_{2k} A_k^{(2)}$$

where the  $Q$ 's refer to the two transitions and are correction factors.

By moving the  $z$ -axis so that it lies perpendicular to the plane of the two detectors (plane formed by  $\vec{k}_1$  and  $\vec{k}_2$ )

the correlation function may be written as

$$W(\theta) = \sum_n B_{2n} \cos(2n\theta) .$$

This form is most convenient for the situation in the present experiment. These have been calculated (e.g. Yates, 1964) or may be measured experimentally using angular correlations for which the factor  $A_k$  are known.

## 2.2 Perturbed Angular Correlation

If the nucleus is subject to a magnetic field  $H$  perpendicular to the plane of the two radiations following the emission of the first gamma ray, its spin will undergo a classical Larmor precession with frequency  $\omega = g\mu_N H/\hbar$  where  $\mu_N$  is the nuclear magneton,  $\hbar$  is Planck's constant divided by  $2\pi$ ,  $g$  is the gyromagnetic ratio of the nucleus in the intermediate state. The angular correlation function for the second radiation emitted a time  $t$  later is then

$$W(\theta - \omega t) . \quad [\text{P.A.C. pg. 96}]$$

If the mean life  $\tau$  of the intermediate state is so short that only an average over  $t$  is observed, then the integral rotation of the angular correlation function is given by

$$\begin{aligned} W(\theta, H) &= \frac{1}{\tau} \int_0^{\infty} \sum_n B_{2n} \cos 2n(\theta - \omega t) e^{-t/\tau} dt \\ &= \sum_n \frac{B_{2n}}{1 + (2n\omega\tau)^2} (\cos 2n\theta - 2n\omega\tau \sin 2n\theta) \end{aligned}$$

The mean precession angle  $\omega\tau$  is measured by

$$\begin{aligned}
 R &= 2 \frac{W(\theta, H) - W(\theta_1 - H)}{W(\theta, H) + W(\theta_1 - H)} \\
 &= \frac{\sum_n \frac{B_{2n}}{1+(2n\omega\tau)^2} 2n\omega\tau \sin 2n\theta}{\sum_n \frac{B_{2n}}{1+(2n\omega\tau)^2} \cos 2n\theta}
 \end{aligned}$$

For measurements made with  $\theta = \frac{3\pi}{4}$  this reduces to

$$R = 2 \frac{\frac{B_2}{1+(2\omega\tau)^2} 2\omega\tau}{B_0 - \frac{B_4}{1+(4\omega\tau)^2}}$$

and for  $\theta = \frac{5\pi}{4}$  becomes

$$R = 2 \frac{\frac{B_2}{1+(2\omega\tau)^2} 2\omega\tau}{B_0 - \frac{B_4}{1+(4\omega\tau)^2}}$$

## CHAPTER III

### FERROMAGNETIC MATERIALS AND HYPERFINE FIELDS

#### 3.1 Introduction

The magnetic field used to perturb the angular correlation pattern may be obtained in two ways. Much work has been and is being done using external fields produced by magnets producing several tens of kilogauss. Matthias, Karlsson and Lerjefors [1962] for example, used external fields of 53.1 and 29.2 kilogauss to measure the shift in the 208 keV-113 keV angular correlation in  $\text{Hf}^{177}$ .

The second method consists of placing the decaying <sup>as</sup> nucleus as an impurity in a ferromagnetic lattice. The hyperfine field acting on the impurity, situated at a host crystal lattice site, is the perturbing field.

The ferromagnetic materials iron, cobalt and nickel are commonly used for this type of experiment since they are ferromagnetic at room temperature and many nuclei of interest may be easily dissolved in concentrations of a few tenths of an atomic percent, in the iron lattice. In these small concentrations, the hyperfine field on the impurity nucleus is unaffected by the presence of the impurities; that is, the hyperfine field is independent of

concentration at low concentrations. In several cases, the field acting on the impurity is quite well known from measurements of radiation from oriented nuclei, nuclear specific heats or from nuclear magnetic resonance and Mössbauer experiments. The systematics of the variation of these fields has been studied to try to understand their origin [Shirley and Westenbarger 1965].

### 3.2 Ferromagnetism

A ferromagnetic substance is one which is said to possess a spontaneous magnetic moment; that is, a magnetic moment even in the absence of an applied field.

A paramagnetic substance is one for which the susceptibility  $\chi = M/H$  is positive. Here,  $M$  is the magnetic moment per unit volume and  $H$  is the magnetic field intensity. Here, by adding some interaction to the paramagnetic situation which tends to line up the ionic magnetic moments in the same direction, one may describe ferromagnetism. In 1907 Weiss postulated such an interaction and accounted for several important features of ferromagnetism. This Weiss field may be considered as equivalent to an effective magnetic field acting on electron spins, and Weiss postulated that its strength should be proportional to the magnetization.

Funkel and Heisenberg pointed out that the physical origin of the Weiss field is in the quantum-mechanical exchange integral. Following certain assumptions [Van Vleck,

1945] it may be shown that the energy of interaction of atoms  $i$  and  $j$ ; having spins  $\vec{S}_i$  and  $\vec{S}_j$  has a term  $E_M = -2J \vec{S}_i \cdot \vec{S}_j$  where  $J$  is the exchange integral and is related to the overlap of the charge distributions  $i$  and  $j$ .

According to the Pauli principle, a change in the relative direction of two spins usually requires a change in the spatial charge distribution in the overlap region. The resulting changes in the coulomb energy of the system may be written as  $-2J \vec{S}_i \cdot \vec{S}_j$  so that it appears as if there were a direct coupling between the two spins.

The temperature dependence of the saturation magnetization may be derived from the Weiss theory, and it is found that, above a temperature  $T_c$ , the Curie temperature, no spontaneous magnetization exists. The spontaneous magnetization, the magnetic moment per atom  $\mu$ , and Curie temperatures are given below for iron and nickel.

	$M_s$ (gauss)	$\mu$ (Bohr magnetons)	$T_c$ ( $^{\circ}$ K)
Fe	1707	2.201	1043
Ni	485	0.606	631 .

At temperatures well below the Curie temperature, the magnetic moments of a ferromagnetic substance are essentially lined up on a microscopic scale. However, the overall moment of the specimen may be much less than that corresponding to saturation since the moments may not be lined up.

Rather, individual domains of aligned moments may be out of line. In this case, an externally applied field will cause alignment of the domains, and produce saturation magnetization.

### 3.3 Hyperfine Fields

A mechanism for the production of the hyperfine field on an impurity atom in the lattice of a ferromagnetic material has been suggested by a number of authors [Marshall, 1958, Watson and Freeman, 1961].

Marshall writes the orienting field in the form

$$H = H_e + H_c + H_a$$

where  $H_e$  = local field at nucleus

$H_c$  = contact field through contact interaction with  
outer s-electrons

$H_a$  = field due to interaction between nucleus and  
electrons around it.

The local field may further be written as

$$H_l = H_e - DM + \frac{4}{3} \pi M + H'$$

where  $H_e$  = external field

$-DM$  = demagnetizing field (dependent on shape of  
sample)

$\frac{4}{3} \pi M$  = Lorentz field

$H'$  = residual magnetic field for non-cubic  
systems

Here,  $M$  is the saturation magnetization quoted previously.

In most cases, the external, Lorentz and demagnetization fields are small and well known. For cubic lattices, the residual field is rigorously zero. The major contribution to the hyperfine field comes from two sources - core polarization, and conduction electron polarization. The  $d$  electrons in the host conduction band spin-polarize the core or conduction  $s$  electrons which hence create a large hyperfine field at the nucleus of the magnetic atom. In general, core polarization is regarded as the largest contributor to the internal field in iron and other 3d magnetic elements.

By definition, internal fields are positive if parallel to the external magnetizing field, and negative if anti-parallel. Also, spin polarization is positive if parallel to the 3d spins which are anti-parallel to the external field.

Spin exchange polarization of the 4s conduction electrons of the magnetic atoms results in a positive contribution to the hyperfine field at the nuclei of these atoms, but also in a negative spin density outside these atoms. This negative spin density can exchange-polarize the  $s$  conduction electrons on a neighbouring (non-magnetic) impurity atom and create a large negative field at the nucleus of that atom. [Watson and Freeman, 1961].

## CHAPTER IV

### THE COLLECTIVE MODEL AND NUCLEAR MOMENTS

#### 4.1 Introduction

There is a considerable body of data available at present concerning ground and low excited states of nuclei. These data have made possible the construction of nuclear models which give good agreement with experimental values of spins, parities and electromagnetic moments of nuclei.

An atomic nucleus consists of an assembly of neutrons and protons confined to a small region of space; the electromagnetic properties of this assembly could be completely described by specifying the current and charge densities of this assembly. However, it is more convenient to describe these properties in terms of electromagnetic multipole moments.

Of these moments, the magnetic dipole and electric quadrupole moments are of interest here. The magnetic dipole moment consists of contributions from the orbital motion of the protons in the nucleus, and from the spins of both the neutrons and the protons. The magnetic dipole operator is then defined by

$$\vec{\mu}_{op} = (\vec{\mu}_{orbital})_{op} + (\vec{\mu}_{spin})_{op} \quad (1)$$

where

$$(\vec{\mu}_{\text{orbital}})_{\text{op}} = \frac{e}{2Mc} \sum_{k=1}^A g_L^{(k)} \vec{L}^{(k)} \quad (2)$$

$$(\vec{\mu}_{\text{spin}})_{\text{op}} = \frac{e}{2Mc} \sum_{k=1}^A g_S^{(k)} \vec{S}^{(k)} \quad (3)$$

$\vec{L}^{(k)}$  and  $\vec{S}^{(k)}$  are the orbital angular momentum and spin operators for the  $k^{\text{th}}$  nucleon, and  $g_L$   $g_S$  are the orbital and spin gyromagnetic ratios.

The magnetic moment is then obtained by calculating the expectation value of the z-component of  $\mu_{\text{op}}$  for the nuclear substate in which the spin is along the z-axis; that is,

$$\mu = \langle J, m=J | \mu_{z_{\text{op}}} | J, m=J \rangle.$$

The electron quadrupole operator is defined by

$$Q_{\text{op}} = e \sum_{k=1}^A g_L^{(k)} (3z_k^2 - r_k^2)$$

where  $g_L^{(k)}$  is formally used to differentiate between protons and neutrons. The electric quadrupole moment is then given by the expectation value of  $Q_{\text{op}}$  for the particular nuclear state.

The actual determination of nuclear moments from any sort of multipole expansion requires the use of wave functions representing the structure of the nucleus. The construction of exact wave functions is prohibitive because it requires full knowledge of the internucleon potential

energy function. Hence, the use of nuclear models is indicated as a means of obtaining approximate wave functions which may be used to calculate nuclear properties.

#### 4.2 The Collective Model

For nuclei in the region of closed shells, the equilibrium shape of the nucleus may be expected to be spherical; far from a closed shell, however, the energetically favourable shape may be non-spherical, and collective motion of shape may modify the nuclear field and become coupled to the motion of the nucleons. A simple description of these nuclei may be given in terms of collective coordinates specifying the shape and orientation of the distorted core. The surface of a figure with a general shape may be written as

$$R = R_0 \left[ 1 + \sum_{\lambda=0}^{\infty} \sum_{\mu=\lambda}^{\lambda} \alpha_{\lambda\mu} Y_{\lambda}^{\mu}(\theta, \phi) \right],$$

where  $\theta$  and  $\phi$  are polar angles with respect to arbitrary axes. Collective motions are expressed by allowing  $\alpha_{\lambda\mu}$  to vary with time. [Preston, pg. 230].

The most important oscillations of such a surface for the case of non-spherical nuclei are those of order 2 associated with ellipsoidal deformation. In this case, the surface may be considered to be axially symmetric about axes fixed in the nucleus and may be written

$$R = R_0 (1 + \beta Y_2^0(\theta))$$

where  $\theta$  is measured relative to the body fixed axes,  $\beta$  is a measure of the deformation, and  $R_0$  is the equilibrium radius.

The nuclear shape may oscillate about its equilibrium shape, or it may rotate while preserving its internal structure, or it may exhibit a combination of oscillation and rotation.

This rotation of the nucleus gives rise to a set of rotational energy levels given by

$$E_{\text{rot}} = \frac{\hbar^2}{2I} \{J(J+1) - J_0(J_0+1)\}$$

where  $J$  and  $J_0$  are the spins of a given level and the ground state respectively. The moment of inertia,  $I$ , associated with the rotational motion is usually much less than the rigid body value since the rotation of the nucleus is not rigid. Such rotational levels have been well identified in the regions  $150 < A < 190$  and  $A > 225$ , both of which are well away from closed shells.

In these regions, where the distortion parameter,  $\beta$ , is large, the nuclear surface will generally be axially symmetric, and the individual particles with total angular momentum  $j$ , will couple separately to the symmetry axis in states characterized by their component of angular momentum  $\Omega_i$  along the symmetry axis.

Because the surface is axially symmetric, the particle states  $+\Omega_i$  and  $-\Omega_i$  are degenerate and particles fill these states in pairs.

The surface may rotate as a whole, and this rotation is characterized by quantum numbers  $J$ ,  $K$  and  $M$ , where  $J$  is the total angular momentum of the surface plus particles,  $K$  is its projection on the body axis and  $M$  its projection of a fixed axis in space. In the ground state, then,  $K = \Omega$ , and  $R$ , the surface angular momentum, is zero (see Figure 2).

For large distortions, the only good quantum numbers are now  $\Omega_i$  and parity, since coupling of different shell model states to the surface may be considerable, and classification of nucleon states according to their  $j$ -values is no longer valid.

#### 4.3 Magnetic Moments

The collective model may be used to compute magnetic moments for deformed nuclei where the shell model is not applicable.

By generalizing equations 1 to 3, the magnetic moment of deformed core plus a single particle may be written

$$\mu = \langle g_s S_z + g_l l_z + g_R R_z \rangle_{M=J} \quad (4)$$

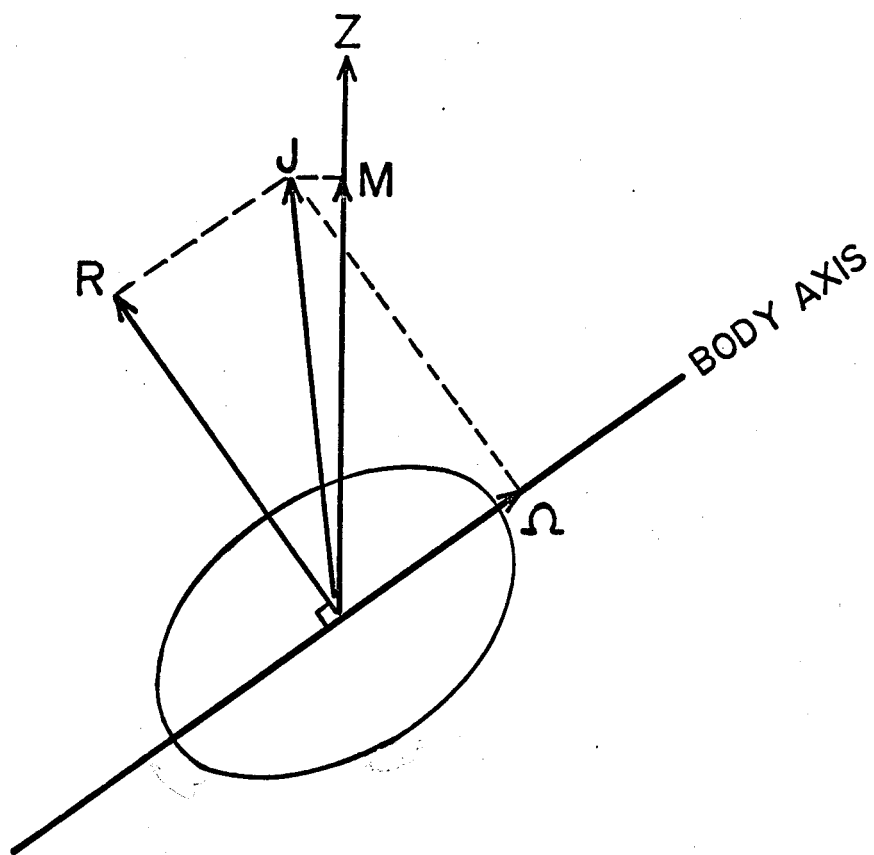
where  $R_z$  is the  $z$  component of angular momentum of the core and  $g_R$  is the corresponding  $g$ -factor.

If the nucleus behaves as a fluid of uniform charge density  $Z/A$ , then

$$g = Z/A .$$

Figure 2

Coupling scheme for highly deformed nuclei



R may be eliminated from equation (4) by writing

$$\begin{aligned}\vec{\mu} &= g_s \vec{S} + g_l \vec{l} + g_R (\vec{J} - \vec{j}) \\ &= g_R \vec{J} + (g_s - g_R) \vec{j} + (g_l - g_s) \vec{l} \\ &= g_R \vec{J} + \vec{G}.\end{aligned}$$

Now, using a wave function  $|JMK\rangle$  with one extra core particle and  $K = \Omega$ ,

$$\begin{aligned}&= \langle JJK | \mu | JJK \rangle = \\ &= \langle JJK | g_R J_z + G_z | JJK \rangle\end{aligned}$$

$\vec{G}$  may be written as a spherical tensor  $G_\mu$

$$\begin{aligned}G_0 &= G_z \\ G_{\pm 1} &= \mp 2^{-(\frac{1}{2})} (G_x \pm iG_y)\end{aligned}$$

In the body coordinate system,  $G_\mu$  becomes

$$G_\mu = \sum_\nu D'_{\mu\nu} G'_\nu.$$

Define a gyromagnetic ratio  $g_k$  by

$$\langle K | G'_0 | K \rangle = K(g_k - g_R)$$

Then, the magnetic moment of the nucleus may be written

$$\mu(J, K) = g_R \frac{J(J+1) - K^2}{J+1} + g_k \frac{K^2}{J+1} \quad K \neq \frac{1}{2} \quad [\text{Preston 331}] \quad (5)$$

and hence,

$$g(J, K) = g_R - \frac{K^2}{J(J+1)} (g_k - g_R)$$

#### 4.4 Multipole Transitions

The magnetic dipole operator may be calculated from expression 4 and written in terms of the spherical tensor  $G_\mu$  [Preston, pg. 340]. The transition rate may be written

$$T(M1) = \frac{16\pi}{9} \frac{k^3}{\hbar} B(M1, J_i K_i \rightarrow J_f K_f)$$

$B(M1)$  is the reduced matrix element for the transition. [Preston, pg. 328]. Within a rotational band, using the previously defined quantity  $g_K$  and the collective gyro-magnetic ratio  $g_R$ , the expression  $\langle K | G_0 | K \rangle = K(g_K - g_R)$  holds. Since, within a band only adjacent levels  $J$  and  $J-1$  are connected by  $M1$ -transitions, the transition rate (for  $K \neq \frac{1}{2}$ ) may be written

$$T(M1) = \frac{16\pi}{9} \frac{k^3}{\hbar} \mu_0^2 (g_K - g_R) K^2 \frac{(J-K)(J+K)}{J(2J+1)} \quad [\text{Preston pg. 340}].$$

where  $\mu_0$  is the nuclear magneton.

In heavy nuclei with large collective quadrupole moments, electric quadrupole transitions are usually very strong. The quadrupole moment operator may be expressed as the sum of a collective term and a term for extra-core particles. The expression involves the deformation parameter  $\beta$  and the average nuclear radius  $R_0$ . Since the value of  $\beta_0$  comes from the irrotational fluid model it is not expected to be extremely accurate, and the quadrupole moment operator is best derived from observed quadrupole moments.

The quadrupole moment is a second rank tensor and by using  $Q_{2\mu}$  and performing an analysis similar to that giving  $B(M1)$ , the  $B(E2)$  reduced matrix element may be written

$$B(E2, J_i K \rightarrow J_f K) = e^2 Q_0^2 (J_i 2K0 | J_f K)^2$$

where  $Q_0$  is the intrinsic quadrupole moment characterizing the nuclear deformation and, for the ground state, is related to the observed quadrupole moment  $Q$  by

$$Q = Q_0 \frac{J(2J-1)}{(J+1)(2J+3)}$$

In terms of the reduced matrix element  $B(E2)$ , the transition probability is

$$T(E2) = \frac{4\pi}{75} \frac{1}{\hbar} k^5 B(E2)$$

The E2 transition rate is enhanced over the single particle rate by the enhancement of the collective over the single particle quadrupole moments. Hence, E2 and M1 transitions may compete, and the mixing ratio is given by

$$\begin{aligned} \delta^2(J \rightarrow J-1) &= \frac{T(E2, J \rightarrow J-1)}{T(M1, J \rightarrow J-1)} \\ &= \frac{3}{20} \left( \frac{\hbar\omega}{mc^2} \right)^2 \left( \frac{Q_0 M^2 c^2}{\hbar^2} \right)^2 \frac{1}{(g_K - g_R)^2} \frac{1}{J^2 - 1} \end{aligned}$$

The transition rates may be written in terms of  $\tau$ , the mean life of the decaying state, the total conversion coefficient  $\alpha_T$  and the mixing ratio  $\delta^2$ . The expressions are

$$T(E2) = \frac{1}{\tau} \frac{1}{1+\alpha_T} \frac{\delta^2}{1+\delta^2}$$

and

$$T(M1) = \frac{1}{\tau} \frac{1}{1+\alpha_T} \frac{1}{1+\delta^2}$$

## CHAPTER V

### APPARATUS

The apparatus involved in this experiment is involved with the detection of gamma rays, and measurement of their energy and time relationship.

The two gamma rays in the cascade discussed previously (Chapter II) must, for the purpose of this experiment be of sufficiently different energy that they may be individually detected. The detectors used are two RCA 6342A photomultiplier tubes with integrally mounted 2 inch by 2 inch sodium iodide crystals. The detector arrangement (crystal plus photomultiplier) is capable of an energy resolution of about 22 percent at the energies used.

The two detectors are mounted on the arms of an angular correlation table, one fixed and one movable, with the faces of the crystals 7 cm. from the axis about which the second detector rotates. The sample being studied is mounted on this axis in one of two manners, depending upon the type of measurement. For an angular correlation, the source (which is on the order of 2 mm. by 3 mm. x 3 mm.) is mounted on a plastic pylon at a height corresponding to the mid-point of the sodium iodide crystals. When the sample is to be magnetically saturated

it is mounted, at the same position, between the poles of a small electromagnet.

The output from the photomultipliers of course contains information about all of the gamma rays being emitted from the decaying nucleus. Most of this information is irrelevant to the purpose at hand and is eliminated by discriminators.

The signal from each photomultiplier is amplified and the signal sent to two discriminators, each of which is set to look at one of the gamma rays in the cascade being studied. [See Figure 3]. The system is adjusted so that discriminators 1A and 2A select one gamma ray and discriminators 1B and 2B the other.

The output from one pair of discriminators selecting both gamma rays (e.g. 1A and 2B) is fed into a fast-slow coincidence circuit. This circuit produces two output pulses. First, if the input from the two discriminators is coincidental, the fast coincidence circuit produces a logic pulse which opens the routing gate, allowing the output from the slow coincidence circuit to register a count on one of the scalers.

In order to eliminate long term instabilities the system is designed to change the direction of the applied magnetic field and the routing of pulses to the scalers automatically (See Figure 4). Thus, when the angular correlation is rotated through an angle of  $\omega T$

Figure 3

Data Collection System

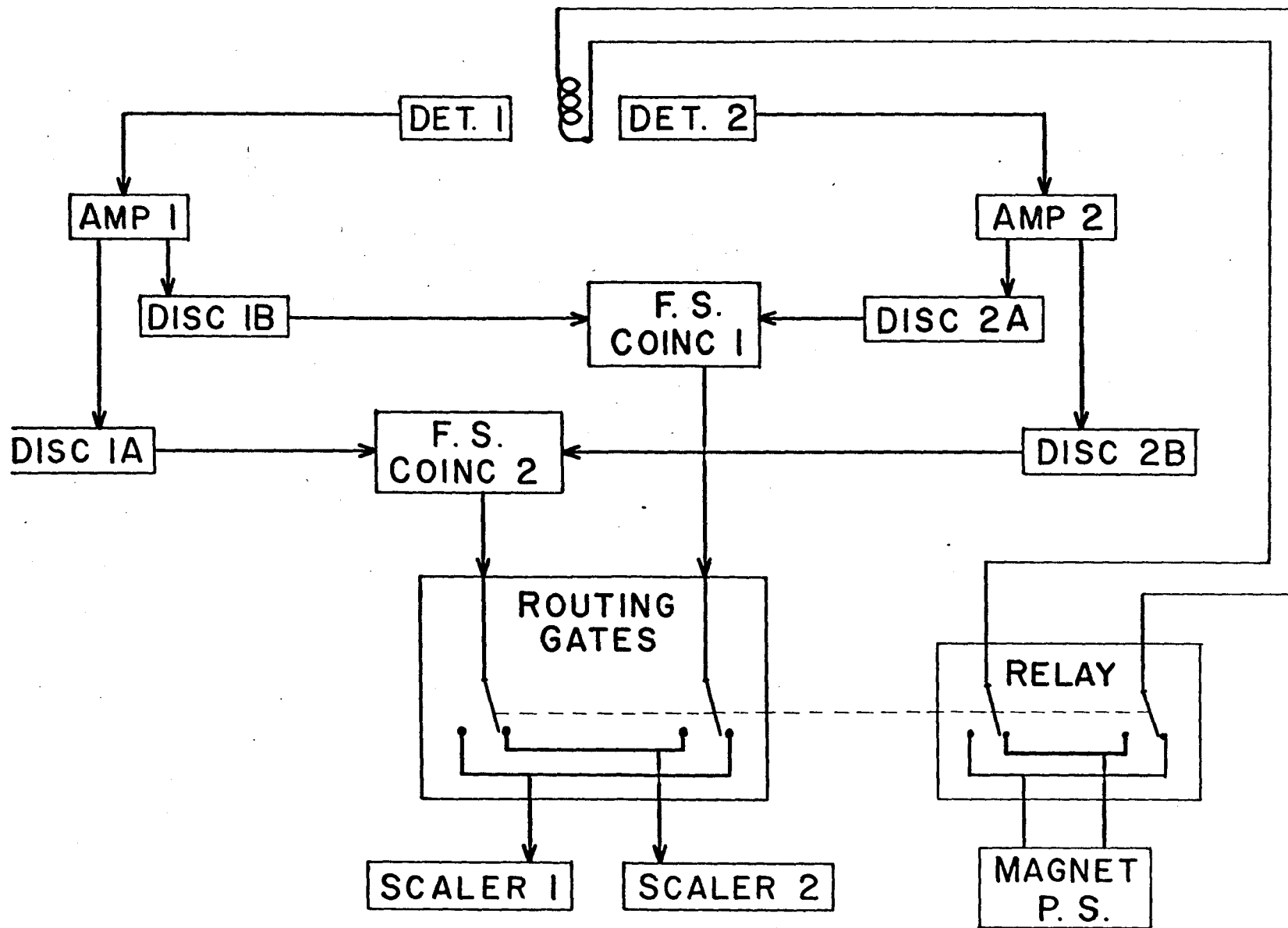
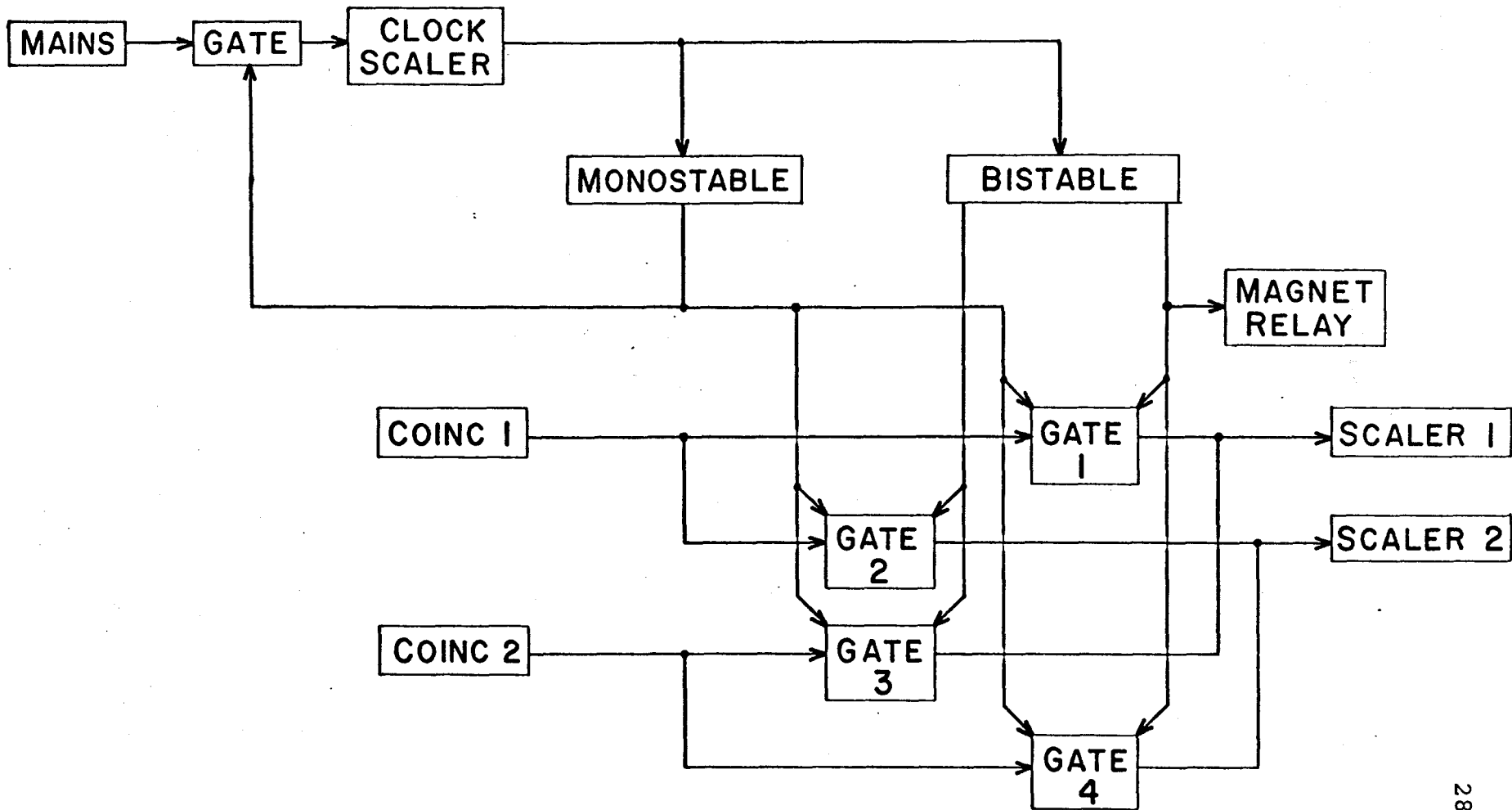


Figure 4

Pulse Routing System



by the field, taking 1B in coincidence with 2A and 1A in coincidence with 2B gives coincidence rates at an angle  $\theta$  which are the equivalent of those obtained from an unperturbed correlation at angles  $\theta \pm \omega\tau$ . Hence, data is accumulated more quickly and short term effects are eliminated. The switch circuit, as may be seen, is driven by a scaler deriving its pulses from the 60 cycle per second mains. After a counting period of about 6 seconds, this scaler stops all the scalers for a time determined by the period of the monostable. During this time (about a quarter of a second) the routing gates and magnetic field are reversed. The system then resumes counting for another period. Because the routing gates are switched also, one scaler continuously counts pulses from the angular correlation rotated to  $\theta + \omega\tau$  and the other scaler counts at  $\theta - \omega\tau$ .

The electromagnet is constructed so that it may be mounted over the axis of the angular correlation table, and produces a magnetic field perpendicular to the plane of the detectors [Murray, 1967]. The magnitude of the field may be varied with the current flowing in the windings, and, at 2 amperes, the field is about 2 kilogauss, which is sufficient to magnetically saturate the sample.

The stabilizing system is designed to correct the gain of the photomultiplier tubes so that a window, set initially over some prominent peak in the spectrum, always

contains that peak.

The photomultiplier tubes are shielded from the fringing field of the electromagnet by magnetic shields made from concentric cylinders of Netic and Conetic AA. [Murray et al. 1967].

Some ancillary equipment was involved in the experiment. A 512 channel analyzer was used to select baselines and window widths for all of the discriminators and single channel analysers and also to obtain the spectra included in Chapter VII.

It was necessary to test the samples used in the electromagnet to ensure that they were being magnetically saturated. To this end two small coils were wound around the sample which was placed between the tips of the magnet poles. Into one of these coils was passed the signal from a sine-wave signal generator. The signal produced in the other coil was monitored with an oscilloscope. Hence, the sample acted as the core in a small transformer. The output from the second coil is dependent upon the state of magnetization of the core until the core becomes saturated, when the amplitude becomes independent of field. Thus, a plot of magnet current versus output amplitude from the second coil can indicate the state of magnetization of the sample.

It is not expected that results obtained at less

than saturation magnetization would be reproducible and if they were, extraction of useful information would be much more difficult.

CHAPTER VI  
EXPERIMENTAL

6.1 Angular Correlations

There were several steps involved in this experiment. First, it was necessary to measure the angular correlation pattern for both the first and second excited states of hafnium. This was done using two different sources; one of  $\text{Lu}_2\text{O}_3$  and one of Lu metal. Both sources were neutron activated in the McMaster reactor, and had activities of about 10 microcuries.

The number of coincidence counts as a function of  $\theta$ , the angle between the two detectors, was found using discriminator windows as shown in Figures 5 and 6. A curve was fitted to these data and the results are given in the next section.

6.2 Sources

The sources for the magnetic perturbation experiments were prepared by ion implantation using the A.E.C.L. Chalk River isotope separator.

Two foils, one of electrolytic iron, and the other of 99.9% pure nickel, were obtained. Their thicknesses were

Fe foil	$0.008 \pm 0.0005$	inches
Ni foil	$0.007 \pm 0.0005$	inches .

The foils were cleaned chemically, then sealed in an

Figure 5

Coincidence spectra showing spectra in coincidence with  
windows A and B

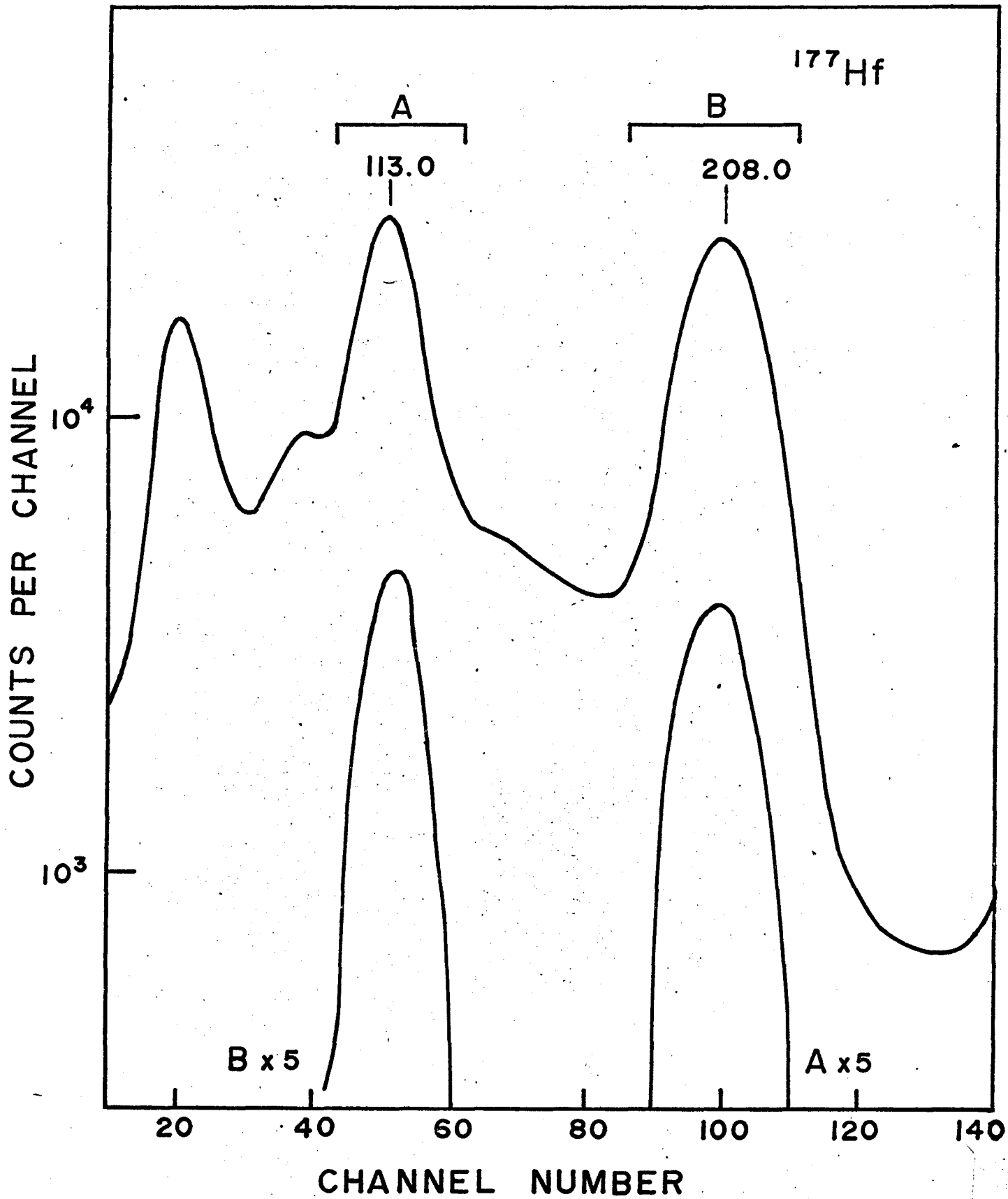
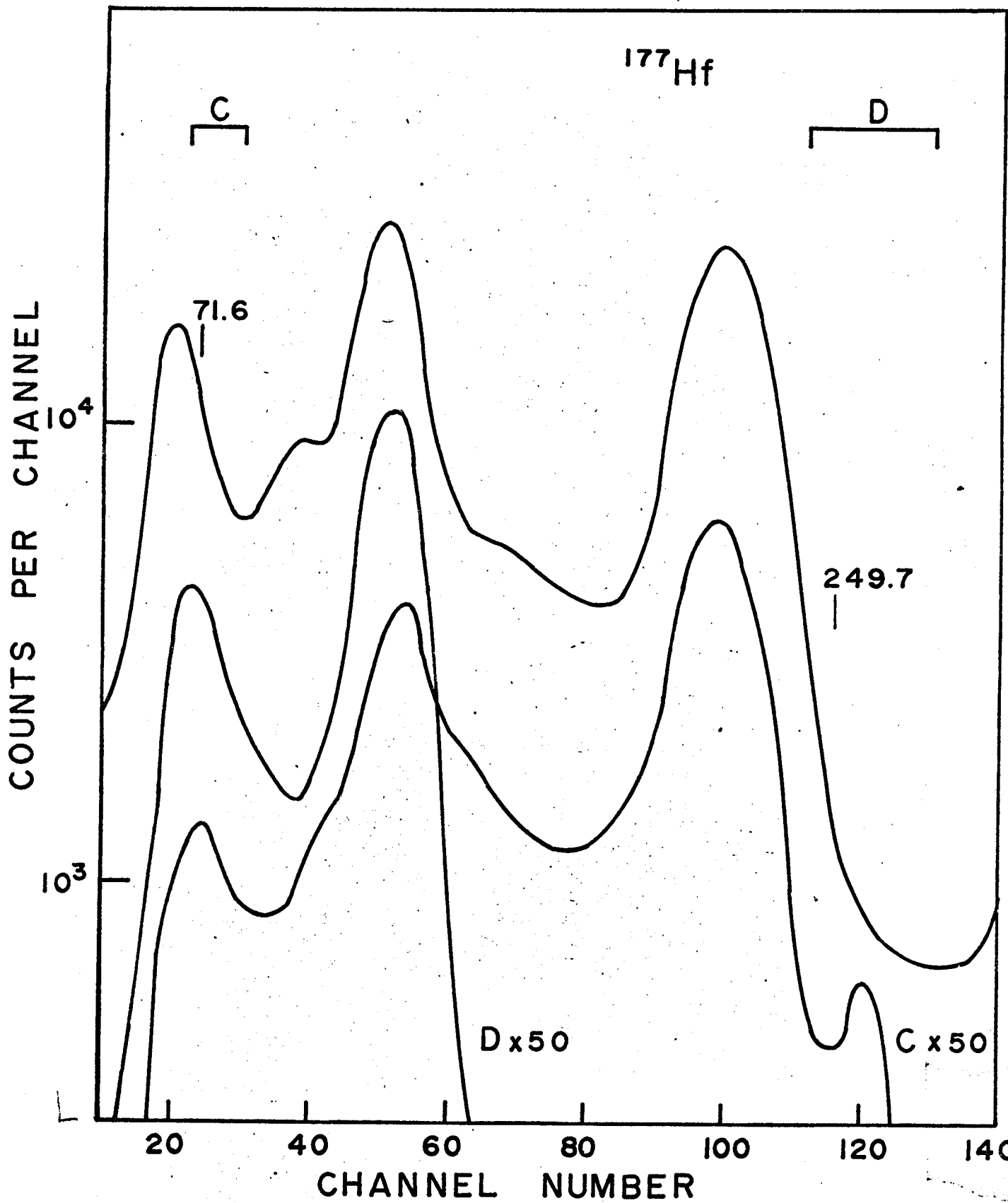


Figure 6

Coincidence spectra showing spectra in coincidence with  
windows C and D

$^{177}\text{Hf}$



evacuated quartz tube and annealed for four hours at 750°C.

For the purpose of mounting in the mass separator, the foils were cut to size (1 cm. x 1 cm.) and mounted with cement on a piece of aluminum sheet about 1/8 inch thick. The foils were mounted so that a beam from the separator about 1.5 cm. by 0.25 cm. could strike both foils at once, placing a line of atoms on the face of the foil.

The resolution of the A.E.C.L. isotope separator was about 0.001 and its transmission was of the same order. A quantity of  $\text{Lu}_2\text{O}_3$  was irradiated in the A.E.C.L. reactor NRX, producing a specific activity of 1.1 millicuries per milligram of  $^{177}\text{Lu}$ . The separator is equipped with connections and a power supply so that some post acceleration may be applied to the ions after they have left the magnet. Hence, it was possible to impart about 70 keV of energy to the  $^{177}\text{Lu}$  ions before they struck the foils. The beam was made by passing  $\text{CCl}_4$  over the hot  $\text{Lu}_2\text{O}_3$  in the ion source, producing  $\text{LuCl}_3$  which is easily ionized.

After the implantation, the foils were removed from the aluminum backing, and the portion containing radioactive nuclei trimmed away. This portion, a strip about 1 cm. by 0.25 cm. was cut into small plates about (0.25 cm. x 0.15 cm.); these plates were glued together to form

a small sample about 0.25 cm. x 0.15 cm. x 0.2 cm. which was placed between the pole tips of the magnet so that the magnetic field was parallel to the largest dimension of the plates. This procedure was followed for both the iron and the nickel foils.

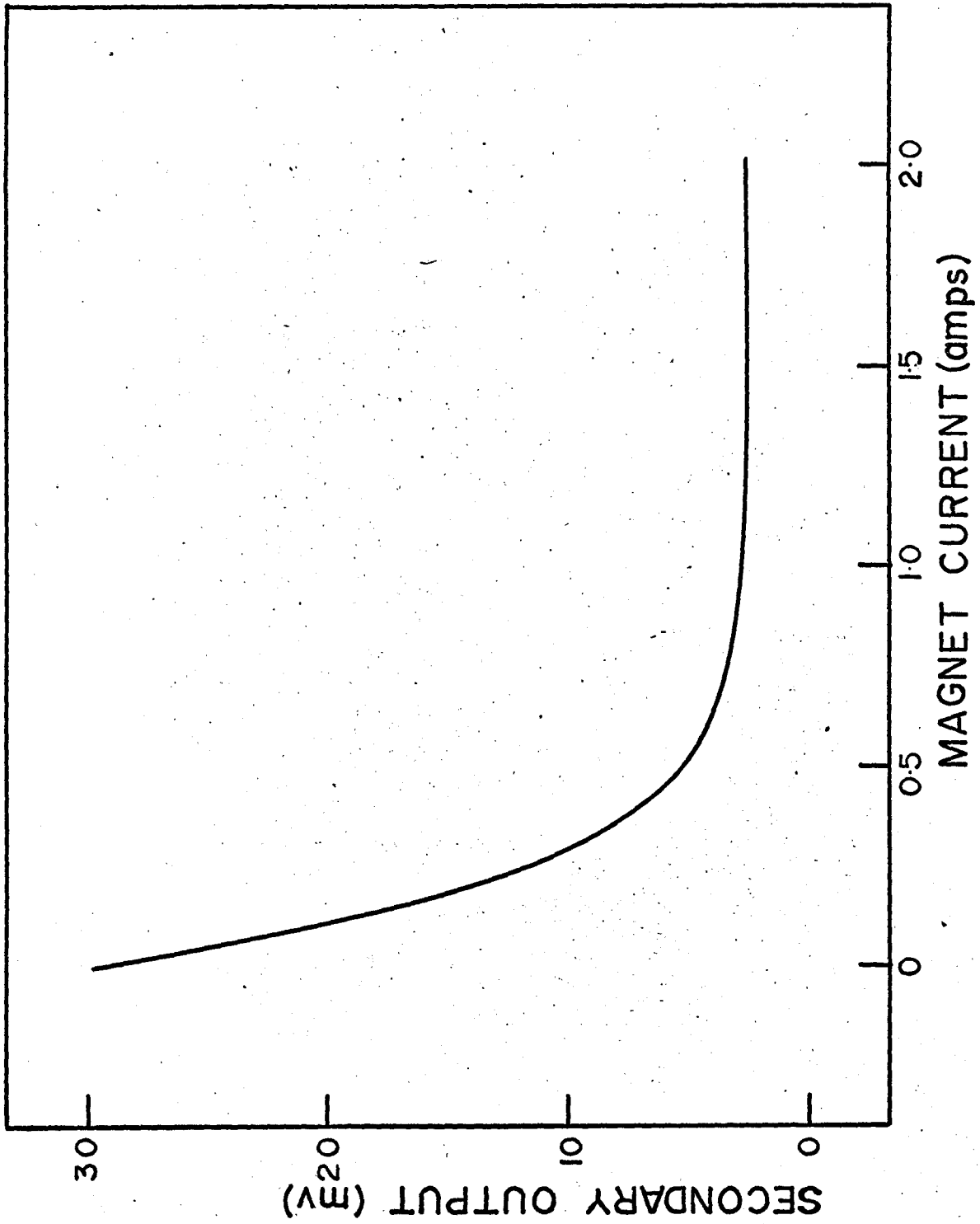
### 6.3 Perturbed Angular Correlations

Now, the measurement of the rotation,  $R$ , was begun, and was performed for the first excited state of  $^{177}\text{Hf}$  for both the iron and nickel foils. Next, the Lu/Fe source was used to measure  $R$  for the second excited state of  $^{177}\text{Hf}$ . After these measurements, the Lu/Fe source was placed in an evacuated quartz tube and annealed in a furnace for 30 minutes at  $900^{\circ}\text{C}$ . After annealing, the measurement of  $R$  for the first excited state was repeated.

The magnetic saturation of the samples was tested and the result for the iron sample is shown in Figure 7. Similar results were obtained for the nickel sample.

Figure 7

Saturation test on the iron sample



## CHAPTER VII

### RESULTS

#### 7.1 Angular Correlations

The angular correlation pattern has been measured for both the 208-113 keV and the 71-250 keV cascades. Using a lutetium metal source, the angular correlation for the former was found to have the form

$$W(\theta) = 1 - (0.101 \pm 0.001) \cos 2\theta$$

which agrees with the results of Matthias, Karlsson and Lerjefors [1962]. The same measurement performed using a  $\text{Lu}_2\text{O}_3$  source gave an attenuated pattern, and  $B_2$  was found to be about 10 percent smaller than the above values.

The angular correlation pattern for the 71-250 keV cascade was found to be

$$W(\theta) = 1 - (0.085 \pm 0.009) \cos 2\theta .$$

These values have not been corrected for the finite solid angles subtended by the detectors or for the presence of other cascades. The errors include statistical uncertainties and allowance for small changes in window positions and width. The decay scheme for the  $^{177}\text{Lu}$  ground state and the angular correlation patterns are given in Figures 8, 9 and 10.

Figure 8

The relevant part of the  $^{177}\text{Lu}$  decay scheme

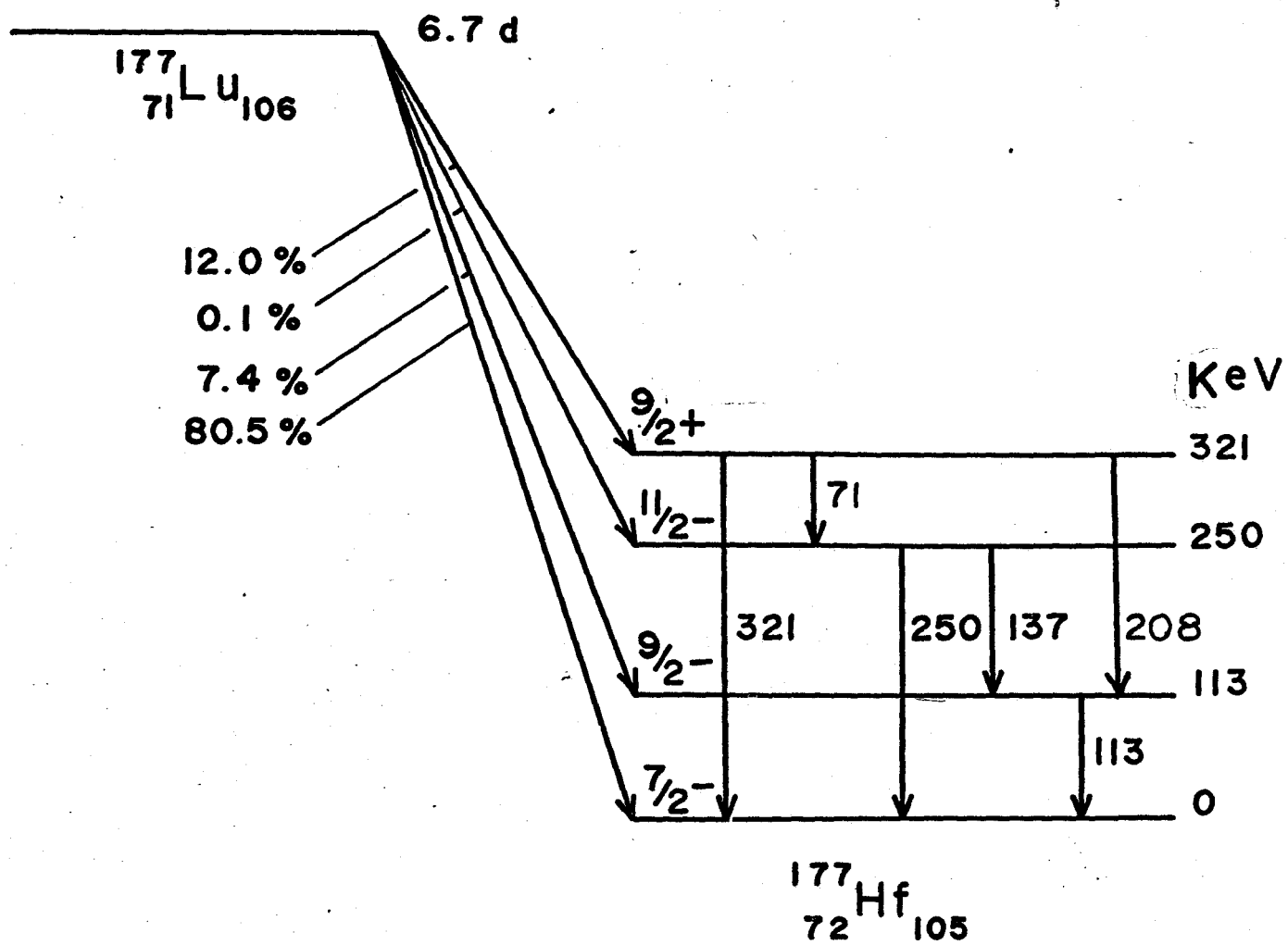


Figure 9

The angular correlation pattern for the 208-113 cascade

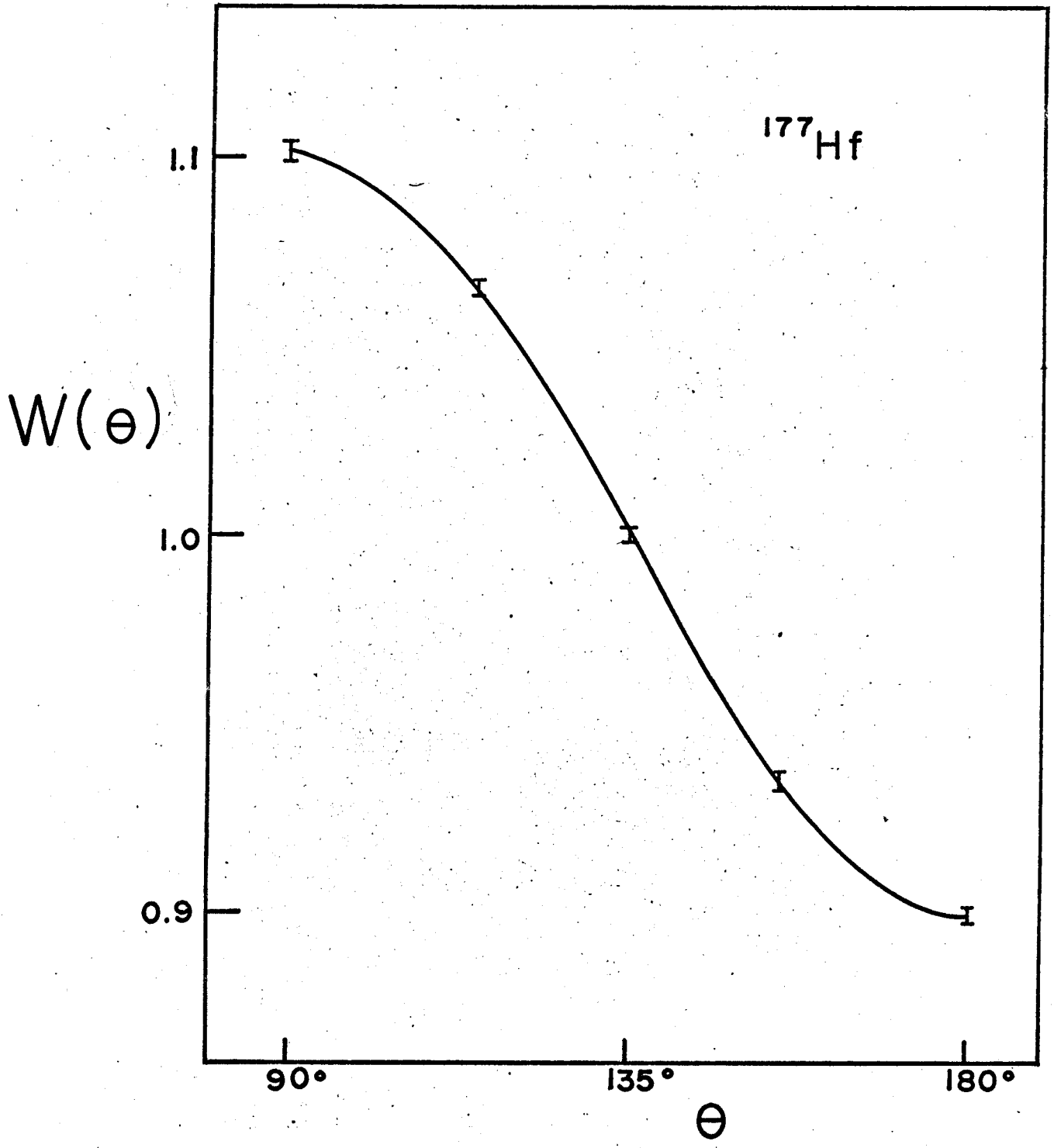
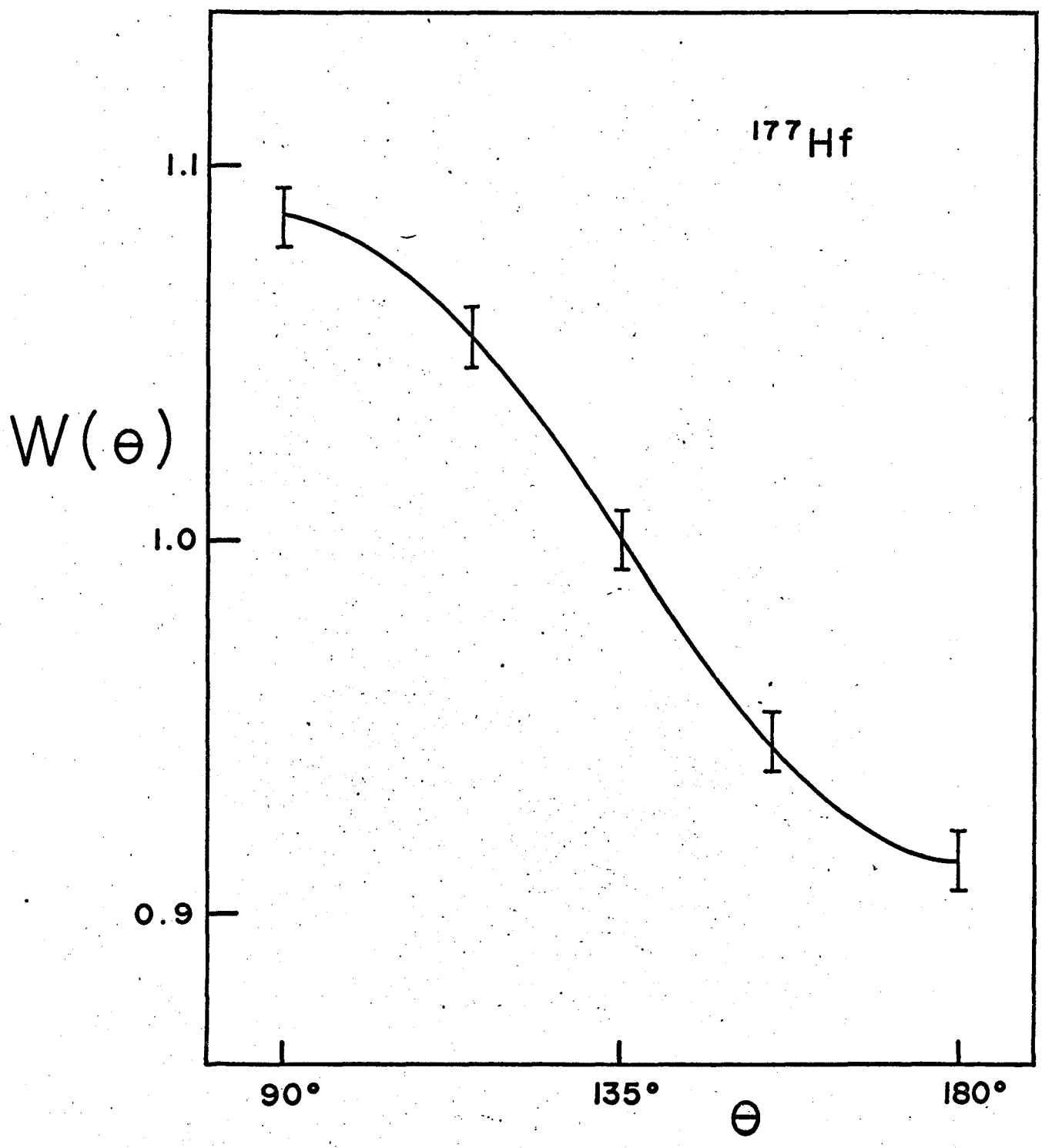


Figure 10

The angular correlation pattern for the 71-250 cascade



## 7.2 Measurement of g-factors

The value of  $R/2$  was measured for these cases: Lu in iron and nickel using the 208-113 cascade and Lu in iron for the 71-250 cascade. The results are given in Table I.

Host	Cascade	$R/2$	$\omega\tau$
Fe	208-113	$0.0219 \pm 0.0008$	$0.104 \pm 0.005$
Ni	208-113	$0.0097 \pm 0.0008$	$0.046 \pm 0.004$
Fe	71-250	$0.0043 \pm 0.0012$	$0.0235 \pm 0.0050$

Because these rotations are small,  $\omega\tau \ll 1$ , and  $\omega\tau$  may be found from the approximation

$$R/2 = \frac{1}{W} \frac{dW}{d\theta} \omega\tau .$$

The values of  $\omega\tau$  satisfy the general relation for  $R/2$ . The magnetic moment of the ground state of  $^{177}\text{Hf}$  has been measured by optical methods and has been found to be

$$\mu = 0.61 \pm 0.03 \quad [\text{Speck, 1956}] .$$

For a spin of  $7/2$ , the magnetic moment gives a g-factor of 0.174.

The g-factor of the  $9/2$ - first excited state has been measured by angular correlation techniques [Matthias, 1962, Manning, 1960] and found to be  $g = 0.235 \pm 0.006$ .

The half-lives of the first two excited states of  $^{177}\text{Hf}$  have been measured:

113 keV level  $T_{1/2} = (0.52 \pm 0.03) \times 10^{-9}$  see [Bird, 1962]

250 keV level  $T_{1/2} = (0.10 \pm 0.02) \times 10^{-9}$  see [N.D.S.] .

By comparing the lifetime of the first and second excited states, and using the measured values of  $\omega\tau$  one may calculate the g-factor for the second excited state from the relation

$$\omega\tau = g \frac{\mu_N}{\hbar} H\tau$$

given in Chapter II. Hence,

$$g_{11/2} = 0.277 \pm 0.080$$

This value does not depend on a calculation of the hyperfine field causing the rotation.

### 7.3 Hyperfine Fields

The internal fields may be calculated by comparing the measured values of  $\omega\tau$  with that measured in an external field. Matthias [1962] used an external field of  $53.1 \pm 0.5$  kOe, and obtained

$$\omega\tau = 0.0416 \pm 0.0020 \text{ rad} .$$

Using this result, and

$$\frac{H_{\text{int}}}{H_{\text{ext}}} = \frac{(\omega\tau)_{\text{int}}}{(\omega\tau)_{\text{ext}}}$$

the value for the internal field on  $^{177}\text{Hf}$  in iron is found to be

$$H_{\text{int}} = -133 \pm 7 \text{ kOe}$$

and that on  $^{177}\text{Hf}$  in nickel is

$$H_{\text{int}} = -58.6 \pm 8 \text{ kOe} .$$

$R/2$  was negative at  $225^\circ$  and positive at  $135^\circ$  indicating that the fields are negative for both alloys.

The rotation of the angular correlation after the iron source had been annealed was measured, and the value obtained was

$$R/2 = 0.001 \pm 0.0007 .$$

## 7.4 Discussion

### 7.4.1 Hyperfine fields

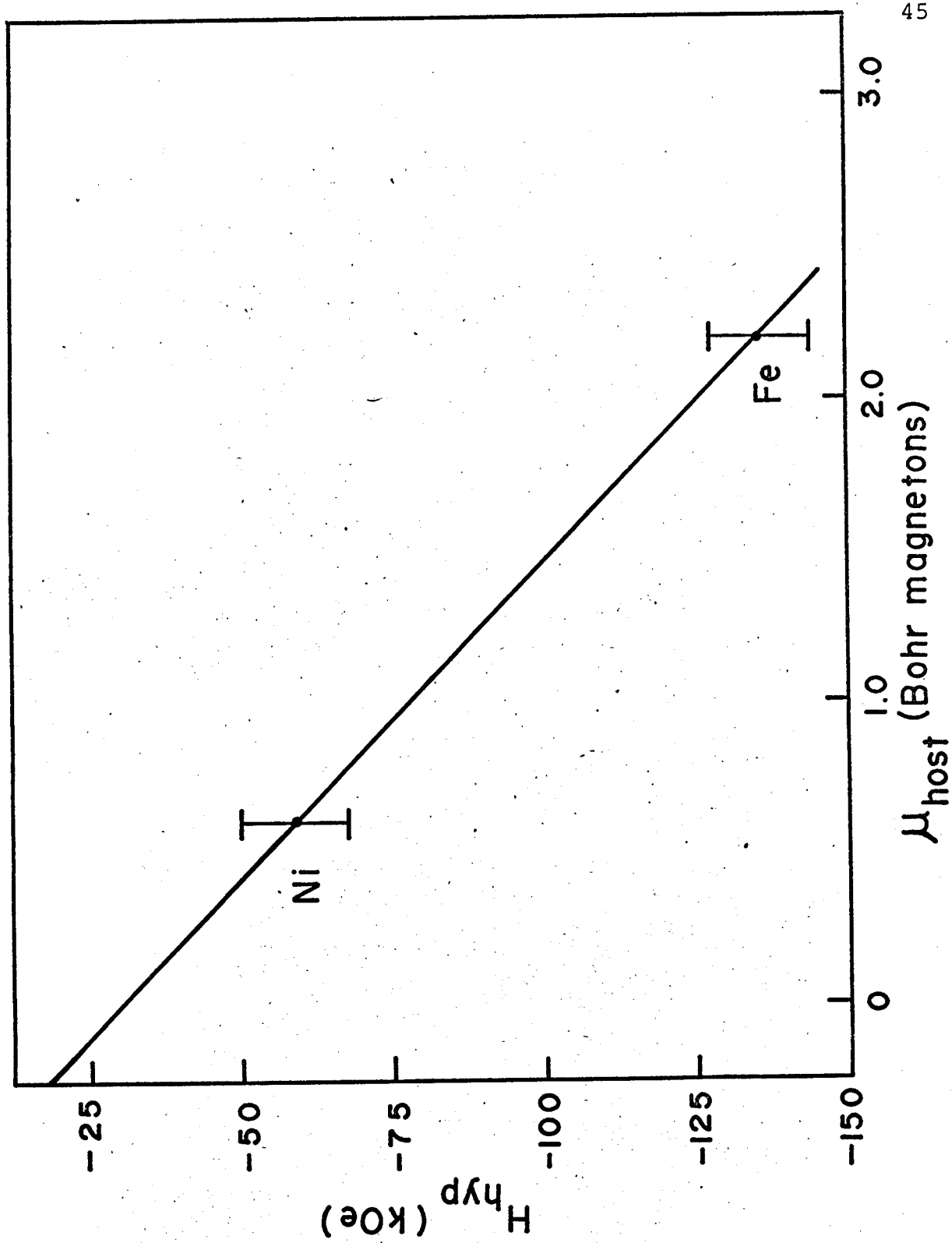
The values obtained for the hyperfine fields acting on a  $^{177}\text{Hf}$  impurity in iron and nickel are given above. These fields are plotted against the host moment in Figure 11. This plot indicates that a relation of the form

$$H_{\text{hyp}} = k\mu_{\text{host}} + H_0$$

where  $H_0$  is a constant may hold for this case. The slope  $k$  is about  $-47 \text{ kOe/Bohr magneton}$ . However, the linear relation is drawn on the basis of only two points, although other evidence has been obtained for such a relation. It has been suggested [Shirley and Westenbarger, 1965, Campbell, 1966] that the hyperfine field appears to be due to two contributions, one proportional to the average host moment and one proportional to the local moment. Thus  $H_0$  could be

Figure 11

Hyperfine field versus host magnetic moment



explained as contribution by the local moment, and is probably the effect of core polarization.

#### 7.4.2 g-factors

The  $^{177}\text{Hf}$  lies in the middle of a region of highly distorted nuclei ( $150 < A < 190$ ), and, hence may be rather well described by the use of the collective model and the strong coupling scheme discussed in Chapter IV. The magnetic moment of a nucleus in the strong coupling approximation is dependent upon two parameters:  $g_R$ , the g-factor corresponding to the angular momentum of the collective rotation, and  $g_K$ , the g-factor appropriate to the angular momentum of the intrinsic particle motion.

Now, using equation 5 of Chapter IV, one may write

$$g(J,K) = g_R + (g_K - g_R) \frac{K^2}{J(J+1)} .$$

This gives three relations for the two parameters  $g_K$  and  $g_R$ . By using the three measured g-factors, and weighting the ground-state and the first and second excited states as 5:5:1 respectively, a least-squares fit to the data was performed. The resulting values of  $g_K$  and  $g_R$  were

$$\left. \begin{array}{l} g_K = 0.123 \\ g_R = 0.346 \end{array} \right\} \text{from least squares} .$$

These two parameters may also be calculated from the known g-factors for the ground and first-excited states.

The results are

$$\begin{aligned} g_K &= 0.126 \pm 0.012 \\ g_R &= 0.343 \pm 0.035 \end{aligned} \quad \text{from } g_{7/2}, g_{9/2}$$

These two sets of values for  $g_K$  and  $g_R$  agree.

It is also possible to obtain a value of  $(g_K - g_R)$  from the transition rates  $T(M1)$

$$\begin{aligned} T(M1)_{9/2 \rightarrow 7/2} &= \frac{1}{\tau_{113}} \frac{1}{1 + \alpha_T} \frac{1}{\delta^2 + 1} \\ &= (1.25 \pm 0.39) \times 10^7 \text{ sec}^{-1} \end{aligned}$$

where

$$\tau_{113} = \text{mean life of 113 keV level} = (0.75 \pm 0.03) \times 10^{-9} \text{ sec}$$

$$\delta = \text{mixing amplitude } E2/M1 \quad \delta^2 = 24 \pm 5 \text{ [N.D.S.]}$$

$$\alpha_T = \text{total conversion coefficient} = 3.27 \pm 0.3 \text{ [N.D.S.]}$$

From results given in Chapter IV, it may be shown that

$$T(M1)_{9/2 \rightarrow 7/2} = 1.8 \times 10^{10} (g_K - g_R)^2$$

$$\text{Using this relation and the value } g_{9/2} = 0.235 \pm 0.010$$

gives

$$g_K = 0.248 \pm 0.090$$

$$g_R = 0.222 \pm 0.080$$

A similar analysis, using  $T(M1)_{11/2 \rightarrow 9/2}$  with

$$\delta^2 = 10^{+14}_{-5}$$

$$\alpha_T = 1.18 \pm 0.12$$

gives

$$g_K = 0.274 \pm 0.100$$

$$g_R = 0.197 \pm 0.090 .$$

Both of these calculations using transition rates yield values for  $g_K$  which are higher than those obtained from measured  $g$ -factors. This difference may be due to errors in the mixing ratios  $\delta$ , or in the total conversion coefficients  $\alpha_T$ .

The  $^{177}\text{Hf}$  nucleus lies in the middle of the deformed region and the intrinsic states of the nucleus are successfully interpreted in the Nilsson scheme (Mottelson and Nilsson, 1953). This scheme uses basis vectors  $|N, \ell, \Lambda, \Sigma\rangle$  where

$N$  = total number of oscillator quanta

$\ell$  = orbital angular-momentum magnitude

$\Lambda$  = component of angular momentum on the symmetry axis

$\Sigma$  = component of spin on the symmetry axis.

For the case of a single extra core particle,

$$\Sigma = \pm \frac{1}{2}.$$

It is possible to calculate  $g_K$  from the Nilsson wave functions [Preston page 265]. Mottelson and Nilsson [1959] classified the ground state of  $^{177}\text{Hf}$  as

$$7/2 - [514]$$

in terms of the basis vectors  $|N\ell\Omega\rangle$  where  $\Omega$  is the component of intrinsic angular momentum on the body axis.

$g_K$  is given by

$$g_K = \frac{1}{2K} (g_s - g_\ell) \sum_{\ell} (a_{\ell, \Omega - \frac{1}{2}}^2 - a_{\ell, \Omega + \frac{1}{2}}^2) + g_\ell$$

where  $g_\ell$  and  $g_s$  are the orbital and spin gyromagnetic ratios for the one extra-core nucleon. In the case, of one neutron,  $g_\ell = 0$  and  $g_s = -3.826$  nuclear magnetons. Nilsson also determined the distortion parameter  $\eta$  to be

$$\eta = 5.5 \quad [\text{Nilsson, 1955}].$$

Using base vectors  $|553+\rangle$ ,  $|533+\rangle$ ,  $|554-\rangle$ , the value of  $g_K$  is found to be  $g_K = 0.44$ . This value is in obvious disagreement with the value calculated from measured  $g$ -factors. Since  $g_K$  determined from Nilsson wave functions depends sensitively on the relative amplitudes in the mixture of wave functions, an attempt to calculate the change in the amplitudes required to give  $g_K$  consistent with the other results was made. It was found that  $a_{54} = 0.784$  and  $(a_{53}^2 + a_{33}^2) = 0.384$  would satisfy  $g_K = 0.127$ . These amplitudes represent a 20% reduction in Nilsson's quoted value of  $a_{54}$  and a corresponding increase in  $a_{53}$  and  $a_{33}$ .

The calculation of  $g_R$  from  $Z/A$  gives  $g_R = 0.41$ . This is considerably larger than the values obtained from the measured  $g$ -factors, in agreement with other work [Bernstein, 1960]. A basic assumption in the derivation of these results is that  $g_K$  and  $g_R$  are unchanged for all levels in the same rotational band and that it is possible to separate the rotational and intrinsic angular momenta.

Thus a possible explanation of the discrepancies between the theoretical and experimental data is that the angular momentum coupling scheme used to derive the expressions for the moments and transition rates gives too rough a description of the physical situation.

Blin-Stoyle [1957] points out that the general trend of nuclear magnetic moments to be between the Schmidt limits may be interpreted as a partial quenching of the intrinsic nucleon moments. This would suggest, for  $^{177}\text{Hf}$ , that the <sup>effective</sup> free neutron moment should be less than the free neutron moment of  $-3.286$  nuclear magnetons.

A more soundly based theoretical suggestion is that the deviation of the static nuclear moment from single-particle estimates may be due to spin-polarization of the even nuclear core by the unpaired extra-core nucleon. Bochnacki and Ogaza [1967] show that, for several nuclei, the ratio of the effective nucleon moment  $g_s^{\text{eff}}$  to the free nucleon moment  $g_s^{\text{free}}$  may be as low as 0.5. The agreement between experiment and this theory indicates that the quenching of the spin  $g$ -factor can be understood in terms of nuclear structure effects; that is, a spin-dependent interaction between nucleons, or spin-polarization.

### 7.5 Summary

The experiment with  $^{177}\text{Hf}$  was intended to measure the internal field on hafnium in iron and nickel and to

measure the g-factor of the 250 keV second excited state.

The results were as follows:

$$H_{\text{Fe}} = -133 \pm 7 \text{ kOe}$$

$$H_{\text{Ni}} = -58.6 \pm 8 \text{ kOe}$$

$$g_{11/2} = -0.277 \pm 0.080$$

The measured g-factor agrees quite well with the value predicted using the g-factors of the ground and first excited states.

However, the value of  $g_K$  derived from the g-factors disagree with the values predicted using the collective model and Nilsson wave functions.

The implantation technique seems to give satisfactory results and should have rather wide applications in allowing studies of materials which do not readily form alloys with ferromagnetic materials.

BIBLIOGRAPHY

- Aeppli, H., Bishop, A.S., Frauenfelder, H., Walter, M.  
and Zunti, W., Phys. Rev. 82, 550 (1951).
- Bernstein, E.M. and De Boer, J., J. Nucl. Phys. 18, 40 (1960).
- Birk, M., Blaugrund, A.E., Goldring, G., Skurnik, E.Z.,  
Sokolowski, S.J., Phys. Rev. 126, No. 2, 726 (1962).
- Blin-Stoyle, R. J., Theories of Nuclear Moments, Oxford  
University Press, London, 1957.
- Bochnacki, Z. and Ogaza, S. Proc. Int. Conf. on Hyperfine  
Interactions, Asilomar, 1967.
- Brady, E. L. and Deutsch, M., Phys. Rev. 72, 870 (1947).
- Campbell, I. A., Proc. Phys. Soc. 89, 71 (1966).
- Deutch, B.I., Hornshoj, P., Nielson, K. Bonde, Boehm, F.,  
Phys. Letts. 21, No. 6, 659 (1966).
- Ferentz and Rosenzweig, appendix 3 in Perturbed Angular  
Correlations, E. Karlsson, E. Matthias, and K. Siegbahn  
ed., North Holland Publ. Co., Amsterdam, 1964.
- Goertzel, G., Phys. Rev. 70, 897 (1946).
- Gschneidner, K. A., Rare Earth Alloys, D. Van Nostrand  
Co. Ltd., Princeton, New Jersey, 1961.
- Hamilton, D. R., Phys. Rev. 58, 122 (1940).
- Hume-Rothery, W., Structure of Metal and Alloys, Institute  
of Metals, London, 1947.
- Manning, G. and Rogers, J.D., Nucl. Phys. 15, 166 (1960).

- Marshall, W., Phys. Rev. 110 (G), 1280 (1958).
- Matthias, E., Karlsson, E. and Lerjefors, C. A., Arkiv for Fysik, 22, No. 8, 139 (1962).
- McMath, T. A., M.Sc. Thesis, McMaster University, 1967.
- Mottelson, B.R., and Nilsson, S.G., Mat. Fys. Skr. Dan. Selsk., 1, No. 8 (1959).
- Murray, J., McMath, T. A., Cameron, J. A., C.J.P., 48, no. 5, 1813 (1967).
- Murray, J., Ph.D. Thesis, McMaster University, 1967.
- Niesen, L., Lubbers, J., Postma, H., de Waard, H., Drentje, S.A., Phys. Letts., 24B, No. 3, 144 (1967).
- Nilsson, S. G., Dan Mat. Fys. Medd., 29, 16 (1955).
- Nuclear Data Sheets, 1961, Natl. Acad. Sci.-Natl. Res. Council, Washington, N.R.C.
- Preston, M.A., Physics of the Nucleus, Addison-Wesley Publishing Co., Reading, Mass., 1962.
- Shirley, D. A. and Westenbarger, G. A., Phys. Rev. 138, (1A), 170 (1965).
- Speck, D. R., Bull. Am. Phys. Soc. Ser. II, 1, 282 (1956).
- Van Vleck, J. H., Revs. Mod. Phys. 17, 27 (1945).
- Watson, R. E. and Freeman, J. A., Phys. Rev. 123(b), 2027 (1961). (1961).
- Yang, C. N., Phys. Rev. 74, 764 (1948).
- Yates, M.J.L., appendix 4 in Perturbed Angular Correlations, E. Karlsson, E. Matthias, and S. Siegbahn, ed., North-Holland Publ. Co., Amsterdam, 1964.